THE HUYGENS DOPPLER WIND EXPERIMENT

Titan Winds Derived from Probe Radio Frequency Measurements

M.K. BIRD[1], R. DUTTA-ROY[1], M. HEYL[1], M. ALLISON[2], S.W. ASMAR[3], W.M. FOLKNER[3], R.A. PRESTON[3], D.H. ATKINSON[4], P. EDENHOFER[5], D. PLETTEMEIER[5], R. WOHLMUTH[5], L. IESS[6] and G.L. TYLER[7]

[1]*Radioastronomisches Inst., Univ. Bonn, Auf dem Hügel 71, 53121 Bonn, Germany*
[2]*NASA-Goddard Institute for Space Studies, New York, NY 10025, USA*
[3]*Jet Propulsion Laboratory, Calif. Inst. of Technology, Pasadena, CA 91109, USA*
[4]*Dept. of Electrical Engineering, University of Idaho, Moscow, ID 83843, USA*
[5]*Institut für Hochfrequenztechnik, Universität Bochum, 44801 Bochum, Germany*
[6]*Dipartimento Aerospaziale, Universitá di Roma 'La apienza', 00184 Roma, Italy*
[7]*Center for Radar Astronomy, Stanford University, Stanford, CA 94305, USA*

Received 30 March 1998; Accepted in final form 20 December 2001

Abstract. A Doppler Wind Experiment (DWE) will be performed during the Titan atmospheric descent of the ESA Huygens Probe. The direction and strength of Titan's zonal winds will be determined with an accuracy better than 1 m s^{-1} from the start of mission at an altitude of ~160 km down to the surface. The Probe's wind-induced horizontal motion will be derived from the residual Doppler shift of its S-band radio link to the Cassini Orbiter, corrected for all known orbit and propagation effects. It is also planned to record the frequency of the Probe signal using large ground-based antennas, thereby providing an additional component of the horizontal drift. In addition to the winds, DWE will obtain valuable information on the rotation, parachute swing and atmospheric buffeting of the Huygens Probe, as well as its position and attitude after Titan touchdown. The DWE measurement strategy relies on experimenter-supplied Ultra-Stable Oscillators to generate the transmitted signal from the Probe and to extract the frequency of the received signal on the Orbiter. Results of the first in-flight checkout, as well as the DWE Doppler calibrations conducted with simulated Huygens signals uplinked from ground (Probe Relay Tests), are described. Ongoing efforts to measure and model Titan's winds using various Earth-based techniques are briefly reviewed.

1. Introduction

The primary objective of the Doppler Wind Experiment (DWE), one of the six scientific investigations comprising the payload of the ESA Huygens Probe (Lebreton and Matson, 1997; Jaffe and Herrell, 1997), is a determination of the wind velocity in Titan's atmosphere (Atkinson *et al.*, 1990; Bird *et al.*, 1997a,b). Measurements of the Doppler shift of the S-band (2040 MHz) carrier signal to the Cassini Orbiter and to Earth will be recorded during the Probe descent in order to deduce wind-induced motion of the Probe to an accuracy better than 1 m s^{-1}. An experiment with the same scientific goal was performed with the Galileo Probe at Jupiter (Pollack *et al.*, 1992; Atkinson *et al.*, 1996, 1997, 1998). Analogous to the Galileo experience (Folkner *et al.*, 1997), it is anticipated that the frequency

Space Science Reviews **104:** 613–640, 2002.

of the Huygens radio signal can be measured on Earth to obtain an additional component of the horizontal winds in spite of the roughly 4-fold decrease in signal level due to the longer free-space propagation distance. Specific secondary science objectives of DWE include measurements of: (a) Doppler fluctuations to determine the turbulence spectrum and possible wave activity in the Titan atmosphere; (b) Doppler and signal level modulation to monitor Probe descent dynamics (e.g., spinrate/spinphase, parachute swing); (c) Probe coordinates and orientation during descent and after impact on Titan.

DWE will complement remote-sensing observations of temperatures and winds from the Cassini Orbiter, providing 'ground truth' for the zonal wind retrievals from the Composite Infrared Spectrometer (CIRS) experiment (Kunde *et al.*, 2002). It is anticipated that the Cassini Radio Science Subsystem (RSS) will provide additional clues about Titan's atmospheric dynamics from their series of radio occultation observations at a variety of latitudes (Kliore *et al.*, 2002). If the Probe descends through regions of turbulence or vertical wave propagation, the Doppler fluctuations will provide information on the associated eddy momentum mixing or planetary waves, respectively. In contrast to the strong radio attenuation in the Jupiter atmosphere inferred from the Galileo Probe signal level measurements (Folkner *et al.*, 1998), propagation effects at S-band for the Huygens DWE on Titan are expected to be negligible (Bird, 1997).

The largest uncertainties in the DWE wind measurement arise from trajectory errors and the stability of the oscillators used to generate the signal on the Probe and receive it on the Orbiter. The desired accuracy can be achieved only with a sufficiently stable radio signal over the duration of the descent. The specified frequency stability of $\delta f/f \lesssim 2 \cdot 10^{-10}$ ($\Rightarrow \delta f \lesssim 0.4$ Hz at S-band) was met by using rubidium-based Ultra-Stable Oscillators in both the transmitter (TUSO) and receiver (RUSO), rather than the standard Temperature Compensated Crystal Oscillators (TCXO).

This paper represents an update to the comprehensive pre-launch instrument descriptions by Bird *et al.* (1997a,b). Some comments on our present knowledge of Titan winds are presented in the next section. An overview of the experimental concept, results from simulated DWE frequency measurements, and a short comparison with the namesake experiment on the Galileo mission are presented in the third section. This is followed by a description of the DWE hardware, the TUSO/RUSO Ultra-Stable Oscillators, and selected DWE results from the cruise phase to Saturn. Included in this latter catagory are the first in-flight checkout 8 days after the Cassini/Huygens launch in October 1997 and a series of Probe Relay Tests (PRTs). It was the first such test (PRT#1) in February 2000 which uncovered anomalous demodulation characteristics of the receiver, eventually leading to a fundamental redesign of the Huygens mission (Lebreton and Matson, 2002). The associated changes in the geometrical conditions, and their obvious consequences for DWE, are incorporated into the present version of the paper.

2. Zonal Winds on Titan

An observational basis for understanding Titan's atmospheric dynamics and meteorology was virtually nonexistent prior to the Voyager 1 flyby on 12 November 1980. Especially valuable information was obtained from infrared (Hanel *et al.*, 1981) and radio science (Tyler *et al.*, 1981) observations. A current review of the dynamic meteorology on Titan, assembled from subsequent studies of the unique Voyager 1 reconnaissance, has been written by Flasar (1998). Coustenis and Taylor (1999) also devote a chapter of their recent book to Titan's atmospheric dynamics and meteorology.

The Doppler tracking data collected during the Voyager 1 occultation were used to derive Titan's vertical temperature-pressure curve (Lindal *et al.*, 1983). Assuming a pure N_2 atmosphere, the temperature was found to decrease with altitude from a surface value of 94 ± 0.7 K to a minimum of $\sim$70 K at the tropopause near 40 km (weak greenhouse effect). A later analysis, including consideration of the uncertainties in mean molecular weight, yielded a surface tempertaure in the range between 92.5 and 101 K (Lellouch *et al.*, 1989). The temperature profile indicated a nearly adiabatic lapse rate below 3–4 km (implying efficient vertical mixing), but a statically stable region at higher altitudes. Vertically propagating gravity waves may exist at heights between 25 and 90 km (Hinson and Tyler, 1983).

Strong zonal winds on Titan ($\sim$100 m s^{-1}) are implied by the latitudinal temperature gradient deduced from the Voyager 1 infrared observations (Flasar *et al.*, 1981; Flasar *et al.*, 1997). Assuming hydrostatic, gradient-balanced flow, the zonal wind velocity u is related to the latitudinal temperature gradient by the 'thermal wind equation':

$$\frac{\partial}{\partial \hat{z}}\left[u^2 \tan\lambda + 2u\Omega a \sin\lambda\right] = -R\frac{\partial}{\partial \lambda}\left[\frac{T}{\mu}\right] \tag{1}$$

where $\hat{z} = \ln(P_s/P)$ is the vertical log-pressure coordinate with P_s the surface pressure, T the temperature, λ the latitude, a the planetary radius, Ω the planetary rotation velocity, μ the mean molecular weight (mass per mole) of the atmospheric gas, and R the gas constant. The second term in Equation (1) can be neglected if $u \gg \Omega a \simeq 11.7$ m s^{-1} (for an assumed Titan rotation period of 16 days), which probably holds until one approaches the surface. In this case the resulting circulation is said to be in cyclostrophic balance. General Circulation Model (GCM) simulations of the Titan regime (Del Genio *et al.*, 1993; Hourdin *et al.*, 1995; Tokano *et al.*, 1999) confirm the likely validity of dynamical scaling assessments (Hunten *et al.*, 1984), and imply that gradient thermal wind balance is an accurate diagnostic of the zonal-mean flow speed.

If the winds are negligible near ground level (e.g., Allison, 1992), Equation (1) may be solved for the zonal wind height profile provided one has knowledge of the temperature with height and latitude. Under these conditions, however, Equa-

tion (1) does not allow one to determine whether the winds are prograde or retrograde.

Integrating Equation (1) upwards, Flasar *et al.* (1997) have derived a model for the zonal wind that increases monotonically to $\sim$100 m s^{-1} in the upper stratosphere at a latitude of $\lambda = 45°$. This model assumes the following equator-to-pole temperature gradients observed at three levels by Voyager 1: $\Delta T \simeq 16$ K at the 0.5 mbar pressure level ($\sim$230 km) from the observations in the 1304 cm^{-1} channel (Flasar *et al.*, 1981; Coustenis, 1990); $\Delta T \lesssim 1$ K at $p = 100$ mbar ($\sim$40 km) from observations at 200 cm^{-1}; and $\Delta T \simeq 2$ K at the surface from the thermal channel at 530 cm^{-1}. Toon *et al.* (1988) have cautioned, however, that these observations may include a significant contribution from stratospheric aerosols. If the IR-observations are stretched to the maximum possible equator-to-pole gradients, corresponding to double the best-fit values (Lunine *et al.*, 1991; Flasar *et al.*, 1997), a zonal wind height profile can be derived with zonal velocities a factor of the order of $\sqrt{2}$ larger than the best estimate. With the additional assumption that the temperature gradient increases roughly linearly with height (i.e., with ln P), Lunine *et al.* (1991) integrated Equation (1) to obtain the following scaled formula for this 'maximum envelope':

$$| u(z) - u_s | \lesssim u_0 \left[1 + \frac{1}{8} \ln[(\frac{P_0}{P(z)}] \right] \cos \lambda \tag{2}$$

where $u_s \simeq 0$ is the wind at the surface, $P(z)$ is the pressure and the wind and pressure at a fiducial height were taken as $u_0 = 200$ m s^{-1} at the $P_0 = 0.5$ mbar level by Lunine *et al.* (1991). The latitudinal dependence in Equation (2) corresponds to superrotation at constant angular velocity ('solid body').

The hypothesized zonal flow on Titan is still a poorly understood regime in the theory of atmospheric dynamics. The meridional and vertical winds, although probably much weaker than zonal motion, are also largely unknown. Only recently have GCMs been adapted to the study of atmospheric superrotation on Titan (Del Genio *et al.*, 1993; Hourdin *et al.*, 1995; Tokano *et al.*, 1999). While these have plausibly simulated an upper atmospheric superrotation qualitatively consistent with the observed temperature gradient on Titan, the detailed wind structure may well depend upon the specific (but as yet undetermined) contributions of the planetary boundary layer and upper level wave propagation, both depending upon the surface characteristics and topography.

Figure 1 shows a summary of what the observations and models imply about Titan's zonal winds. The zonal wind height profile is plotted at $\lambda = 19°$N, which is the latitude corresponding to the originally designated Huygens target on Titan. Subtle differences in the theoretical profiles occur for the new target latitude of $\lambda = 10.7°$S, but the general trend, a roughly linear increase with height, is maintained. The latitude-adjusted profile derived from the Voyager 1 observations by Flasar *et al.* (1997) is shown by the short-dashed curve in Figure 1. The solid line is the corresponding 'maximum envelope' at this latitude given by Equation (2). The

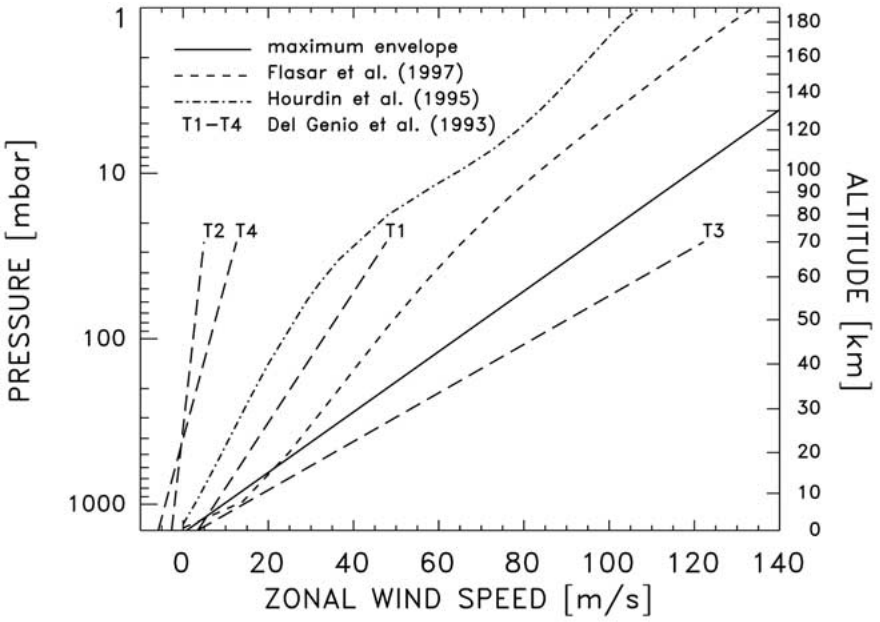

Figure 1. Models of zonal wind height profiles on Titan at a latitude of 19°N. The curve given by the short-dashed line is the integral of the thermal wind equation, using equator-to-pole temperature contrast at various heights inferred from Voyager 1 infrared observations (Flasar *et al.*, 1997). The solid curve is a 'maximum envelope' (Lunine *et al.*, 1991) assuming upper bounds on the Voyager temperature gradients. The dash-dotted curve is a prediction from a specifically developed Titan circulation model (Hourdin *et al.*, 1995). The long-dashed curves labeled 'T1-T4' are linear fits to four atmospheric simulations for a planet rotating at the Titan period (16 days) performed by Del Genio *et al.* (1993) over a more limited range of altitudes. T1: model with a global absorbing cloud at altitudes from 20–40 km; T2: same atmospheric simulation, but without an absorbing cloud; T3: T1 without stratospheric drag; T4: T1 with greatly weakened surface drag.

dash-dotted curve is a mean of the northern winter solstice and northern spring equinox models of Hourdin *et al.* (1995), which is valid for the Huygens epoch in January 2005. Also plotted in Figure 1 are linear fits to the results of a Titan dynamical process study using a terrestrial atmospheric GCM incorporating various idealizations of the stratification and drag likely to be relevant to the planet's specific circulation regime (Del Genio *et al.*, 1993; long-dashed lines T1–T4). The baseline Titan-like scenario (T1) features an optically thick ($\tau \simeq 5$), statically stable cloud layer in the upper troposphere, slowed down to a 16-day planetary rotation period. The assumed thick cloud merely serves the purpose of imposing a strong upper atmospheric static stability in the adapted Earth model, as apparently required for an equatorial convergence of eddy momentum flux by barotropic eddies. Running the GCM code to equilibrium, one obtains zonal-mean flows of several tens of meters per second up to the maximum simulated altitude level near 100 mbar. The flow regime is supported by the horizontal mixing of quasi-barotropic eddies. The other curves in Figure 1 are the baseline Titan model of

Del Genio *et al.* (1993), but with the following modifications: (T2) without the absorbing global cloud, (T3) without stratospheric drag, and (T4) with negligible surface drag. The implication is that T1 agrees best with the winds inferred from the Voyager 1 observations (Flasar *et al.*, 1981) as well as with the model prediction of Hourdin *et al.* (1995). The more recent calculations by Tokano *et al.* (1999) predict a very weak prograde zonal wind at the designated Huygens target latitude of only a few m s^{-1} in the troposphere and probably less than 20 m s^{-1} near the start of the descent at ($h \sim 170$ km). Evidently, the absorbing global cloud, stratospheric drag and surface drag are all essential ingredients of superrotational circulation on Titan.

Evidence for winds on Titan was also derived from ground-based photometric measurements recorded during the occultation of the relatively bright star 28 Sgr (Hubbard *et al.*, 1993). A latitudinal profile, presumed symmetric about the equator, was inferred from the shape of isopycnic surfaces in the stratosphere (0.25 mbar level). The zonal flow varied from $\sim$80 m s^{-1} near the equator to more than 170 m s^{-1} at 60° latitude.

Infrared heterodyne observations of Titan's ethane emission in the 12 μm band, which originates near the 1 mbar level ($\sim$200 km altitude), have been used to estimate Titan zonal wind speeds (Kostiuk *et al.*, 2001). The Doppler shift of a given C_2H_6 line is measured when the telescope's field-of-view is centered on the east and west limbs of the Titan disk, respectively. The frequency difference between the line centers of these two spectra should be twice the Doppler shift expected from the mean zonal flow velocity. The results provide strong evidence that Titan's zonal winds are moving in the direction of planetary rotation (*prograde*). Using data from three separate observation opportunities at the NASA/IRFT at Mauna Kea (1993, 1995–1996), the combined statistical probability that the winds are prograde is 94%. The wind speeds derived from simple models for the hemispheric mean measurements are high, but with an almost equally high uncertainty. Assuming solid body rotation, a mean equatorial zonal wind speed of 250 ± 150 m s^{-1} is retrieved, which implies an atmospheric rotation period of $\sim$19 h.

The traditional cloud-tracking technique to derive winds has been frustrated in the case of Titan by the virtual absence of contrast in the Voyager 1 images. Using a large amount of image processing, one attempt to measure winds from atmospheric features was performed (Wenkert and Garneau, 1987). Many near-infrared images of Titan have been obtained with the refurbished planetary camera (WF/PC2) of the Hubble Space Telescope (HST) during the 1994–1995 oppositions. Careful processing of the 14 images from 1994 revealed a large bright surface feature in the leading hemisphere (Smith *et al.*, 1996). Although some structure in the WF/PC2 images is suggestive of atmospheric condensations (Lorenz *et al.*, 1995; 1999; Caldwell *et al.*, 1996), a confident cloud-tracking determination of wind vectors has not yet emerged.

Subsequent observations of Titan using adaptic optics at the ESO 3.6-m telescope in LaSilla (Combes *et al.*, 1997) and the near-infrared camera (NICMOS)

on HST (Meier *et al.*, 2000), failed to detect short-term changes in albedo that might be attributed to cloud activity. In spite of the general lack of contrast in the Titan atmosphere from imaging observations, anomalous infrared spectra have been recorded (Griffith *et al.*, 1998) that are best explained by transient low-level clouds (∼15 km altitude) occupying about 10% of the observed disk. More recent observations (Griffith *et al.*, 2000) now reveal variations on shorter time scales (hours to days) in the 2.11–2.17 μm spectral region sensitive to CH_4 cloud reflection. These new measurements are best simulated by clouds at higher altitudes (∼25 km) that cover typically 0.5% of the moon's disk.

The GCM experiments and the few available observations suggest that planetary atmospheric circulation such as Titan's may be maintained by 'potential vorticity' mixing (Allison *et al.*, 1994). To the extent that this approaches the zero potential vorticity (ZPV) limit for a stable symmetric circulation about the equator, a maximum envelope can be derived for the latitudinal wind profile:

$$u_{max}(\lambda) = (u_e + \Omega a)\,(\cos\lambda)^{\frac{2}{R_i}-1} - \Omega a \cos\lambda \tag{3}$$

with u_e the equatorial zonal velocity and R_i the Richardson number. Equation (3) implies that u_{max} increases with latitude for the large values of R_i appropriate for a statically stable stratosphere, consistent with the Titan zonal wind profile derived by Hubbard *et al.* (1993), at least for latitudes from the equator to the maximum jet at 60°. A vertical profile for $R_i(z)$ could be determined from a combination of DWE wind and HASI (Huygens Atmospheric Structure Instrument: Fulchignoni *et al.*, 1997) temperature/pressure measurements at one latitude. Global remote sensing observations from the Cassini Orbiter would then provide an elegant test of the applicability of the ZPV constraint.

3. DWE Experimental Strategies

3.1. TITAN TARGETING

Successful execution of the DWE depends critically on the experiment geometry and sequence of events during Titan descent. In order to measure the presumably dominant zonal wind component, it is essential that the respective positions of Probe and Orbiter provide a favorable projection of the East-West wind drift motion onto the Probe/Orbiter line-of-sight. As mentioned earlier, telemetry demodulation problems discovered in the Huygens receivers on the Cassini Orbiter have resulted, after an in-depth analysis of the link performance, in a major redesign of the Huygens mission (Lebreton and Matson, 2002). Of particular concern to DWE was the rearrangement of the Huygens mission geometry required to reduce the Doppler shift of the Probe-Orbiter radio link.

According to the current planning, the Huygens Probe mission will no longer occur on the first, but rather the third targeted Titan flyby. The new mission date

has been moved back to 14 January 2005, about 6 months after arrival at Saturn. A backup opportunity with very similar geometrical conditions, but with increased fuel expenditure and extended delay for returning to the Cassini Saturn Tour, could be arranged for the subsequent Titan flyby 32 days later. The Probe will now be separated from the Orbiter on Christmas Day 2004, only 20 days prior to entry into Titan's atmosphere. Two days later, a deflection maneuver will bring the Orbiter into a retrograde flyby trajectory that passes 'left' of Titan at a minimum altitude near 65 000 km, rather than the originally planned flyby at 1200 km on Titan's 'right' side. The Orbiter Delay Time (ODT), previously set at 4 h, will now be 2.1 h after Probe entry.

Probe and Orbiter targeting at Titan can be visualized on the Titan disk from a direction defined by their asymptotic approach velocities, the so-called *B-plane* (see also Bird *et al.*, 1997b; Sollazzo *et al.*, 1997). Figure 2 shows a B-plane projection with the Probe and Orbiter targets at Titan at the time of Probe entry. The asymptotic velocity vector defines the direction of the S-axis, passing through the center of Titan perpendicular to the B-plane, and its unit vector $\hat{S}$. The B-plane passes through the center of Titan and is spanned by the T- and R-axes. The T-axis is defined by the intersection of the B-plane with the Titan equatorial plane. In other words, the direction of the unit vector $\hat{T}$ along the T-axis is defined by the cross product $\hat{S} \times \hat{P}$, where $\hat{P}$ is a unit vector in the direction of Titan's rotational axis, positive northward. The R-axis and associated unit vector complete the orthogonal system: $\hat{R} = \hat{S} \times \hat{T}$.

The concentric circles centered on the origin denote values of constant Probe entry angles in the Titan atmosphere. Maintaining a balance between peak and integrated heat flux on the front shield, an optimum entry angle of $\gamma = -64^\circ$ was derived from atmospheric entry simulation studies. The B-plane azimuth angle was originally selected as $\theta_P = -60^\circ$, which mapped on Titan to latitude 19°N, longitude 152°W at the start of the descent. The target delivery accuracy, defined by the 3σ targeting error ellipse, was formerly ± 480 km $\times \pm 150$ km, corresponding to $\pm 3.3^\circ$ in latitude and $\pm 11.2^\circ$ in longitude. The targeting ellipse corresponding to the revised mission, utilizing navigation data from two previous Titan flybys, is smaller (± 306 km $\times \pm 35$ km). Utilizing additional optical navigation data, the Orbiter would have been more accurately targeted to a point that yielded an altitude of closest approach at 1200 km at the azimuth angle $\theta_O = -22.6^\circ$ (Sollazzo *et al.*, 1997). The semi-axes of the Orbiter targeting ellipse were 174 km $\times$ 39 km.

An essential component of the Huygens mission recovery was to reduce the Doppler shift of the radio link. Because the velocity magnitude could not be significantly changed, the only feasible way to accomplish this was to greatly increase the Orbiter flyby distance. Without reiterating the intermediate steps in the redesign process, it suffices here to note that the optimum Orbiter B-plane azimuth for a high-altitude flyby was determined to be $\theta_O = -180^\circ$, i.e. passing through the negative T-axis of the B-plane. The Orbiter B-plane target, however, is well out of the picture shown in Figure 2 (flyby altitude $\sim$65 000 km). In order to maintain

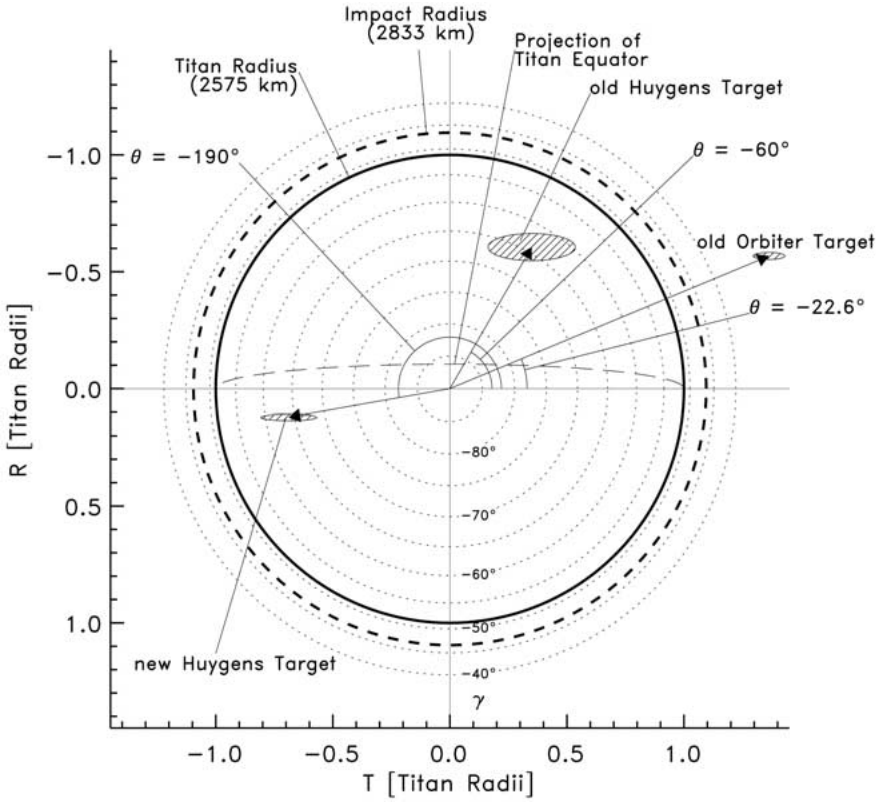

Figure 2. Huygens Probe and Cassini Orbiter targets in the Titan B-plane. The concentric circles denote loci of constant Probe entry angles in the Titan atmosphere from center disk ($\gamma = -90°$) to $\gamma = -40°$. Probe entry is optimized at $\gamma = -64°$. In the original mission plan, the Probe target was in the upper right quadrant and had a relatively large error. The Orbiter was formerly targeted for a flyby altitude at 1200 km, in the same quadrant. Retaining $\gamma = -64°$, the new Probe target was moved around to the left in order to optimize the radio link performance for the new Orbiter flyby trajectory at azimuth angle $-180°$.

satisfactory link performance with the Orbiter now on the left side of Titan, it was necessary to retarget the Probe to a point in the same hemisphere. The optimum entry angle of $\gamma = -64°$, governed by the entry thermal budget, was not changed. An optimum B-plane azimuth was determined to be $\theta_P = -190°$, yielding an atmospheric entry point on Titan at latitude 10.7°S, longitude 199°W. The Titan rotation axis will now be tilted away from the incoming Probe by 6.0° (angle between $\hat{P}$ and $-\hat{R}$). The trace of the Titan equator on the disk is shown in projection onto the B-plane in Figure 2.

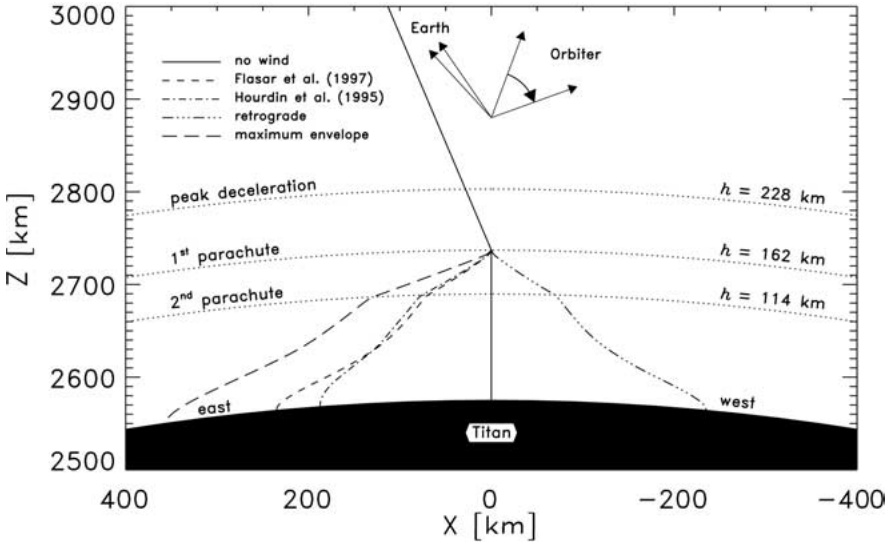

Figure 3. Huygens nominal descent trajectory for various zonal wind models. The diagram shows the path of the Probe, viewed from the north, as it is blown in longitude by the east/west winds. It is assumed that the winds affect the Probe's position only after deployment of the first parachute at an altitude $h \simeq 162$ km. The descent velocity increases when the second (smaller) parachute is deployed at $h \simeq 114$ km. Prograde (retrograde) winds cause eastward (westward) drift. Depending on the strength of the winds, the Probe touchdown on Titan can be many hundreds of kilometers from the atmospheric entry point. The projected directions to Orbiter and Earth over the course of the descent are indicated.

3.2. PROBE MOTION DURING DESCENT

The nominal Huygens entry/descent trajectory for various zonal wind models is depicted in Figure 3. As the Probe enters the Titan atmosphere, it is subjected to a deceleration of the order of 13 g at an altitude $h \simeq 228$ km. A first parachute is deployed at a speed near Mach 1.5 ($h \simeq 162$ km), marking the beginning of the descent phase (time $= t_0$). Slowing to subsonic velocity, the heat shield is jettisoned and transmission of data is initiated (at $t = t_0 + 150$ s). The radio signal will be recorded both on the Orbiter and on Earth in the directions indicated. The Probe then falls at the terminal velocity governed primarily by the ballistic coefficient of the Probe parachute system. It is assumed that the Probe also drifts in longitude with the east/west winds, remaining at a roughly contant latitude for negligible north/south winds. The large initial parachute is released at $t = t_0 + 15$ min ($h \simeq 114$ km) and replaced by a smaller drogue parachute in order to decrease the descent time. The time constant for the Probe velocity to adjust for changes in the winds will decrease toward lower altitudes due to the increasing atmospheric density (Bird *et al.*, 1997b). In the case of the maximum envelope profile (s. Figure 1), the Probe touchdown on Titan will be about 360 km east of the atmospheric entry point. The zonal drift will produce a small shift in the apparent direction

to Earth as shown in Figure 3. This drift also affects the apparent position to the Orbiter. The larger shift in direction shown in Figure 3 (clockwise ~50°), however, is caused by its apparent motion toward the horizon along the high-altitude flyby trajectory.

The (first order) Doppler shift measured on the Orbiter is given by:

$$\Delta f = -\frac{f}{c}\,\Delta V \tag{4}$$

$$\Delta V = \left(\vec{V}_P - \vec{V}_O\right) \cdot \vec{R}_{OP} \tag{5}$$

where $\vec{V}_P$, and $\vec{V}_O$ are the Probe and Orbiter velocities, respectively, and $\vec{R}_{OP}$ is a unit vector from Orbiter to Probe (radio ray path):

$$\vec{R}_{OP} = \frac{\vec{R}_P - \vec{R}_O}{\mid \vec{R}_P - \vec{R}_O \mid} \tag{6}$$

Higher order Doppler, special relativistic, and gravitational red shift terms can be neglected (Atkinson *et al.*, 1998).

The sign of ΔV is negative at the beginning of the Titan descent, so that the received frequency is increased (blue shifted) from Equation (4). In the Titan-centered frame, the ray path projection of the Probe velocity consists of 4 contributions:

$$\vec{R}_{OP} \cdot \vec{V}_P = V_1 + V_2 + V_3 + V_4 \tag{7}$$

where the four terms are sensitive to Probe motion as follows:

$V_1 \sim$ zonal wind u (positive toward East)
$V_2 \sim$ Titan rotation $\Omega a \cos\lambda$ (co-aligned with V_1)
$V_3 \sim$ meridional wind v (positive toward North)
$V_4 \sim$ descent velocity v_T + vertical wind w (positive upwards)

and the Orbiter's velocity projection onto the radio ray path is:

$$\vec{R}_{OP} \cdot \vec{V}_O = V_5 \tag{8}$$

The term V_1, the drift velocity due to zonal winds, is the measurement of interest to DWE. This will be either parallel or antiparallel to the velocity V_2 from Titan rotation, the magnitude of which is assumed to be $\Omega a \cos\lambda \simeq 11.6$ m s^{-1} at $\lambda = -10.7°$. The meridional drift term V_3 would be indeterminate without the additional Doppler measurement from Earth. It is expected to be small ($v \ll u$) except perhaps in the last few kilometers above the surface. The vertical velocity V_4 must be determined independently using measurements of height from the Probe's proximity sensor and/or HASI temperature/pressure data.

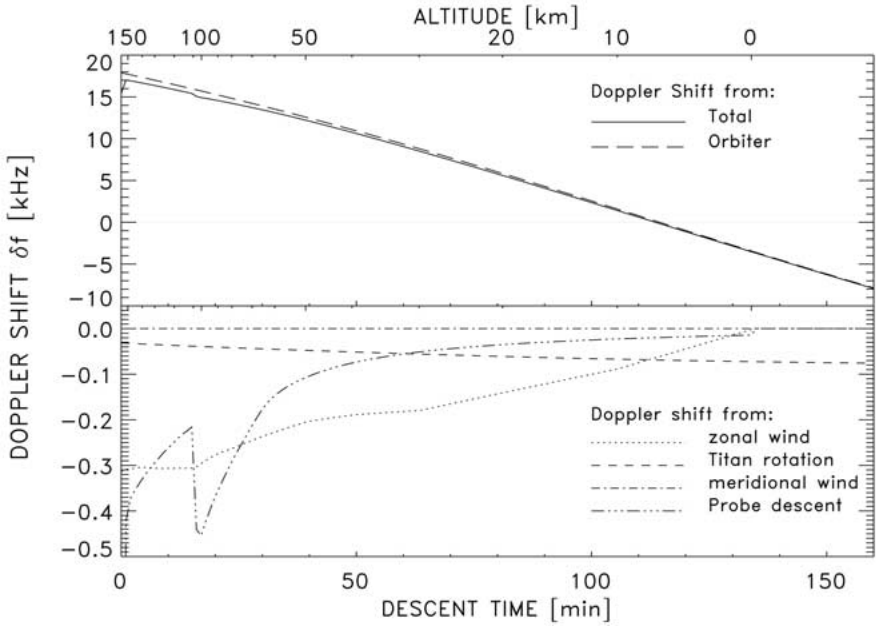

Figure 4. Doppler shift contributions for the nominal Huygens descent profile. Upper panel: The solid line is the total Doppler shift between Probe and Orbiter. Most of the Doppler shift comes from the relative motion of the receiver (Orbiter) with respect to line of sight to the Probe (dashed line). Lower panel: The velocity components of the Probe in the Titan atmosphere: eastward zonal drift (dotted line), planetary rotation (dashed line), southward meridional drift (dot-dashed line), and vertical descent (triple-dot-dashed line), are all expected to produce a frequency decrease (red shift) from the Probe motion *away from* the Orbiter.

The eventual uncertainty in the zonal wind velocity will be sensitive to any measurement error in the descent velocity V_4. This was an especially serious problem for the Galileo Probe, for which the line-of-sight to the Orbiter was very nearly vertical (Pollack *et al.*, 1992; Atkinson *et al.*, 1998). Assuming that the Huygens descent velocity can be determined to the estimated accuracy of 1% (Bird *et al.*, 1997b; Fulchignoni *et al.*, 1997), the associated uncertainty in the zonal wind speed will be about 2 m s^{-1} (20 cm s^{-1}) near the beginning (end) of the descent.

Figure 4 presents the expected time profiles of the five line-of-sight Doppler contributions in Equations (7) and (8) for the nominal Huygens descent (duration: 135 min). The upper panel shows the total Doppler shift between Probe and Orbiter (solid line). It is clear that most of the Doppler shift comes from the motion of the Orbiter projected along the line-of-sight to the Probe (dashed line). The Doppler shift from other individual motions of the Probe in the Titan atmosphere are plotted at higher resolution in the lower panel. The curves are for eastward zonal drift (dotted line), planetary rotation (dashed line), southward meridional drift (dot-dashed line), and vertical descent (triple-dot-dashed line). All of these are expected to produce a frequency decrease (red shift) from their motion *away*

from the Orbiter. The discontinuity at $t = 15$ min, most prominant in the descent velocity, marks the exchange of parachutes. The 100% nominal zonal wind model $u(z)$ (Flasar *et al.*, 1997; see also Figures 1 and 3) was used for computing the zonal wind contribution V_1. The minor contribution from Titan rotation (V_2) slowly increases during the descent as the radial projection of the zonal motion becomes more favorable. The new geometry for the Huygens DWE at Titan yields an almost negligible Probe/Orbiter line-of-sight projection for the meridional component V_3. A nominal velocity of $v = -1$ m s^{-1} was used in Figure 4, but even substantially higher velocities would not be measureable because of the small projection onto the line-of-sight.

Independent determinations of Probe horizontal drift may be available near the surface from either (a) proximity sensor measurements utilizing pendulum swing motion, or (b) successive images from the Descent Imager & Spectral Radiometer (DISR: Tomasko *et al.*, 1997). These would provide a helpful comparison with the DWE height profile just prior to touchdown where the horizontal winds may well be weak. It is hoped that DWE measurements will continue after impact on Titan to provide a reliable absolute frequency reference for zero wind.

3.3. Parallels with the Galileo doppler wind experiment

The main scientific goal of the namesake experiment performed during the Galileo Probe mission at Jupiter on 7 December 1995 (Atkinson *et al.*, 1996; 1997; 1998) was very comparable to that of the Huygens DWE. It is remarkable that this is one of the few obvious similarities between the two investigations. As demonstrated in Table I, there are distinct differences in the instrumentation and experimental geometry. Whereas the Galileo DWE observed an L-band signal from a rapidly-changing vantage point with only a small Doppler component for the zonal motions, the Huygens DWE will be recording an S-band signal with a significant and constantly increasing component in the zonal direction. The Galileo Probe's carrier signal was also successfully recorded at radio telescopes on Earth (Folkner *et al.*, 1997), which was located in a direction nearly orthogonal to the Probe-Orbiter line. Although this viewing geometry was ideal for measuring zonal winds, it was also far away from the axis of the Probe's antenna, which, of course, was pointed at the Orbiter. The resulting extremely low signal levels meant that these frequency measurements could be retrieved only upon implementing a sophisticated signal extraction process to deconvolve the phase modulation from the raw spectral recordings.

Zonal winds at Jupiter were observed to be prograde, strong and surprisingly uniform $\sim$160–180 m s^{-1} at levels between 4 and 20 bars, thereby suggesting an absence of strong meridional temperature gradients at the deep, weakly stratified levels sounded by the Galileo Probe (Atkinson *et al.*, 1997; 1998). There was evidence for slowing down at higher levels, where the zonal flow should merge with the velocities measured for the visible clouds. Independent accelerometer

TABLE I
DWE Comparison: Huygens/Cassini and Galileo Probe

Parameter	Galileo Probe	Huygens/Cassini
Probe Relay Link:		
frequency band	L	S
chain A/B frequency (MHz)	1387.0/1387.1	2040.0/2097.1
Doppler shift, $\Delta V = 1$ m s^{-1} (Hz)	4.62	6.80
RF power (W)	23	10
polarization A/B	LCP/RCP	LCP/RCP
signal source A/B	USO/TCXO	TUSO/TCXO
data rate (bits/s)	128	8192
USO		
output frequency (MHz)	23.117	10.000
warm-up time (hours)	<6	<0.5
drift stability $\Delta f/f$ (30 min)	$1.73 \pm 0.09 \times 10^{-9}$	2×10^{-10}
Probe Antenna		
type/size	cup/0.254 m	helix/0.17 m
gain (dBi)	9.8	5
3 dB-beam Ø (°)	56	120
Orbiter Antenna		
parabolic antenna Ø(m)	1.09	4.3
gain(dBi)	21.0	34
3 dB-beam Ø (°)	12.6	2.6
PRL Receiver		
local oscillator A/B	USO/USO	RUSO/TCXO
Doppler recording rate (Hz)	1.5	8
signal power recording rate (Hz)	21.3	8
Doppler resolution (mHz) [mm s^{-1}]	181 [39]	48 [7]
signal power resolution (dBm)	0.01	$\simeq$0.05
DWE Geometry		
entry angle (°)	-8.38	-64 ± 4
entry velocity (km s^{-1})	47.8	5.7
maximum entry deceleration (g)	228	13
entry latitude (°)	6.53 N	10.7 S
entry longitude (°)	4.46 W	199 W
mission duration (min)	57.64	135 ± 15
Probe aspect angle (°)	2–14	25–70
planet rotation velocity	12.6 km s^{-1}	11.6 m s^{-1}

TABLE II
Earth Reception of Galileo Probe and Huygens

Parameter	Galileo Probe	Huygens
Frequency band	L	S
Frequency (MHz)	1387.0	2040.0
RF power (W)	23	10
Probe antenna gain to Earth (dBi)	−4	4
Distance to Earth (AU)	6.2	8.1
Receiving antenna	VLA	NRAO 100-m
Receiving diameter (m)	130	100
Receiving efficiency	0.5	0.7
Receiving noise temperature (K)	34	30
Received voltage SNR in 1-second	4.9	5.5

measurements from the Galileo Probe Atmospheric Structure Instrument agreed with the DWE results (Seiff *et al.*, 1997). On Titan, however, strong vertical shears are likely to be an important feature of a statically stable and differentially heated atmosphere. *In situ* verification of these thermal winds by the Huygens DWE could be extrapolated to a global scale from Orbiter observations of the horizontal temperature contrast using the techniques established by the Voyager IRIS experiment (Flasar *et al.*, 1981).

3.4. Ground-based measurements of Titan winds

Ground-based observations of the Huygens Probe to support the DWE will be made at one or two large radio antennas. With the current nominal trajectory, the Probe mission on Friday, 14 January 2005, will occur in the ground received three-hour time interval starting at about 09:11 UT. This will be shortly after culmination, for example, at the Very Large Array in New Mexico or the Deep Space Network (DSN) complex in California (the DSN 70m antennas are presently not equipped to track the Probe signal, because their standard S-band receivers do not cover the Probe's transmission frequency). Another available ground-based station would be the new NRAO 100-m antenna at Green Bank, WV/USA, which would have visibility of the Huygens Probe at least at the start of descent. The expected signal strength is even somewhat better than for the Earth-based observation of the Galileo Probe. Key parameters in the link budget for the Galileo and Huygens Earth-based Doppler measurements are compared in Table II. Saturn's mean distance from Earth is roughly twice that of Jupiter, but the additional free-space loss for the experiment at Titan is only 2.3 dB rather than the expected 6 dB. This is because the Huygens DWE will be performed at opposition, in contrast to the Galileo Probe

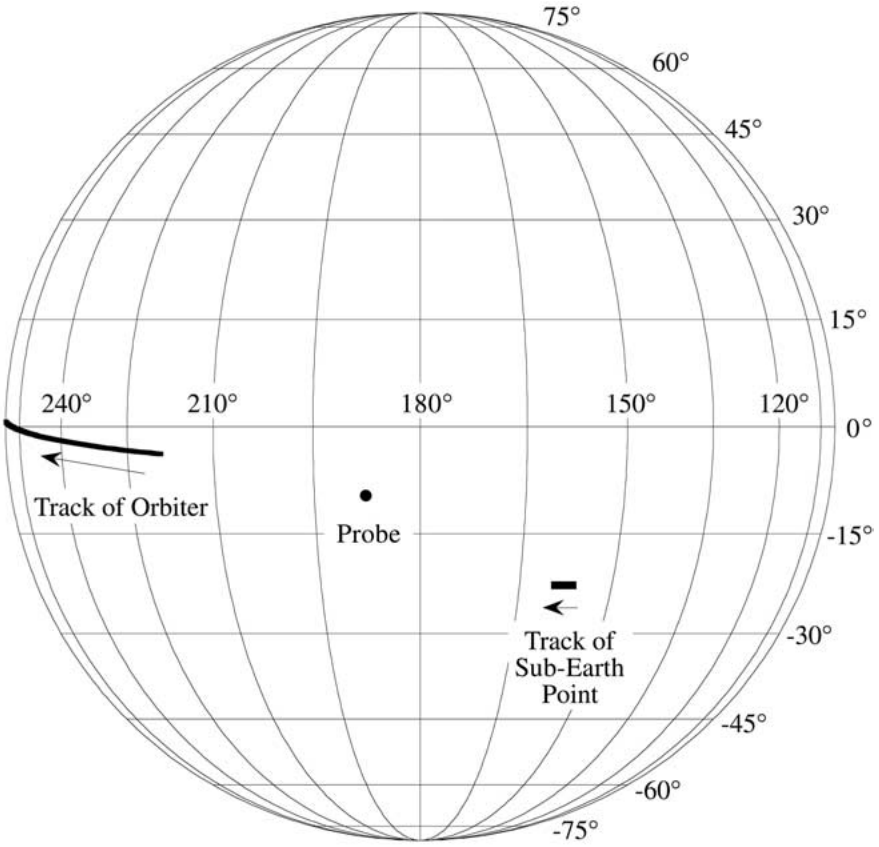

Figure 5. Geometry for DWE wind measurements Probe-to-Orbiter and Probe-to-Earth in a Titan-fixed coordinate frame. The projected positions of Probe, Orbiter, and Earth are plotted on the Titan surface for the time of the nominal mission on 14 January 2005. The Probe position remains constant for the no wind case assumed here. The sub-Earth and sub-Sun points, indistinguishable at this scale on this date of solar opposition, drift westward due to Titan's rotation. The Probe–Orbiter projection is aligned essentially along the zonal (E-W) direction. The Probe-Earth projection is slightly inclined to the Probe-Orbiter projection, thereby making it more sensitive to possible meridional motion.

experiment conducted at almost maximum Earth range near solar conjunction. An important factor is the comparative transmitter antenna gain in the direction to Earth, which is within the 3 dB beam and thus distinctly more favorable for the Huygens geometry at Titan than for the Galileo Probe at Jupiter. Probe motion due to rapid planetary rotation, which carried the Galileo Probe beyond the planetary limb and further degraded the effective radiated power toward Earth, will not be a problem for the Huygens DWE.

The relevant geometry for the Titan wind measurements is shown in Figure 5 for the nominal Huygens mission. Titan, orbiting Saturn at a constant distance of 20.4 Saturn radii, is located fairly close to Saturn's noon meridian on this date.

The sub-Earth and sub-Sun points are virtually identical because Saturn is exactly at opposition. The ground tracks of the Cassini Orbiter, Huygens Probe and sub-Earth points are shown in a Titan body-fixed coordinate system from a viewpoint above the intersection of Titan's equatorial plane with the Titan anti-Saturn meridian (180°). It is assumed in this plot that the Probe descends straight down in the body-fixed frame (no winds). The trajectory of the Orbiter projects to a point northwest of the Probe and moves during the mission in northwesterly direction. The Probe-Orbiter Doppler shift measures primarily the Probe zonal velocity (after removing the vertical motion). The Probe-Earth Doppler basically detects the same Probe motion in reverse, but with a slightly larger admixture of meridional velocity. Although angular separation of the two Doppler measurement directions is not near the optimal 90°, the two measurement sets could still allow for separation of the zonal and meridional winds.

In spite of the improvement over the Galileo Probe experiment, the strength of the Huygens signal will still be too weak to detect directly at the Earth antennas because the signal is strongly modulated by the (then) unknown telemetry. Instead, wide-band recordings of the Probe signal will be made during the three-hour Probe descent. After the Probe telemetry is relayed to Earth by the Cassini Orbiter, the recorded signal would be processed against a model of the telemetry, enabling signal integration over several seconds for the Probe carrier frequency measurements.

4. DWE Instrumentation

4.1. END-TO-END CONCEPT

DWE is the only Huygens investigation with instrumentation on both Probe and Orbiter (part of the Probe Support Equipment – PSE). Figure 6 shows a block diagram of the DWE measurement from start to finish. The DWE-TUSO drives the signal generated by the Transmitter A, one of the two redundant radio links. The carrier signals of the radio links are separated in frequency (A: 2040 MHz; B: 2097.1 MHz) and polarization (A: LCP = left circularly polarized; B: RCP = right circularly polarized). An internal TCXO oscillator drives link B and another TCXO serves as back-up on link A in case of TUSO failure during cruise. The final selection of oscillators on link A will be made a few days prior to Probe–Orbiter separation. The TUSO output signal at 10 MHz is upconverted to 2040 MHz and transmitted to the dedicated Probe Support Avionics (PSA) Receiver A on the Orbiter via the Cassini High Gain Antenna (HGA). Cruise checkouts, which are conducted approximately every six months, enable continuous monitoring of the DWE components and radio subsystem. At Titan the signal is amplified for free-space transmission via the Probe transmitter antenna. Receiver A is tuned to the nominal Transmitter A output frequency at 2040 MHz in checkout mode ($f_{ref} = 0$) and is shifted by $f_{ref} = +38.5$ kHz for descent mode.

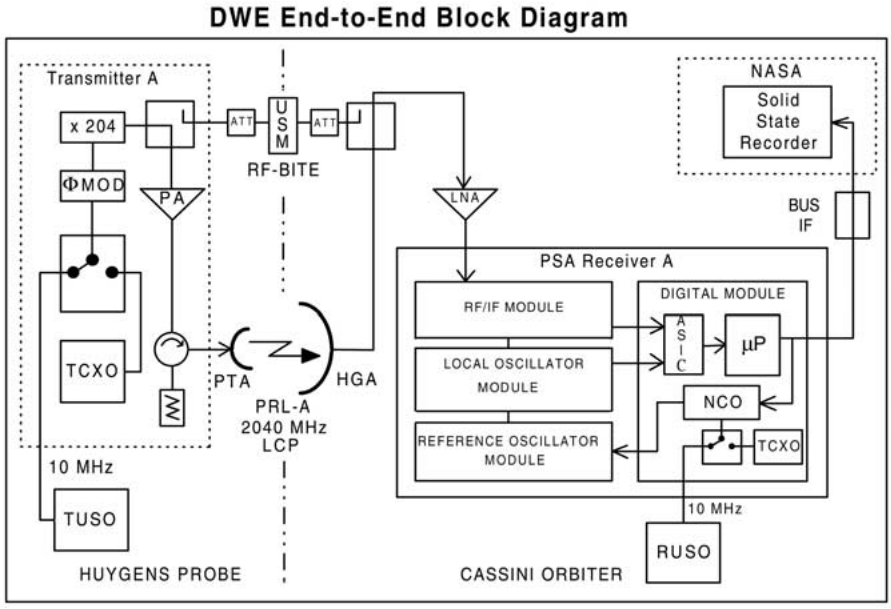

Figure 6. DWE experiment configuration (reprinted from Bird *et al.*, 1997b).

Timing and signal generation in PSA-A are controlled by the DWE-RUSO. Switching to a back-up TCXO is possible in case the RUSO fails. Phase-lock loop control in the receivers is governed by a numerically controlled oscillator (NCO), the output of which provides the DWE frequency measurement at 8 samples per second. The signal level is monitored in parallel at the same sample rate. The TUSO will be powered well before the initial transmission from the Probe (as much as four hours head start), in order to warm up and achieve the required frequency stability. The RUSO has a much more favorable thermal environment and will be switched on about one hour before the start of data reception.

4.2. Transmitter and receiver USO programs

The DWE ultrastable oscillators, the first rubidium oscillators used in a deep space mission, were developed and constructed by Daimler-Benz Aerospace – DASA, Satellite Systems Division (now: Astrium Telecommunications), Ottobrunn, Germany. The DASA design concept was built around a Rb-resonator in a 'physics package' supplied by Efratom Elektronik GmbH.

The required fast warm-up time and insensitivity to the mechanical loads expected during the Huygens entry phase were the major drivers in the selection of a rubidium ultrastable oscillator. The DWE instrument specification imposed a requirement for a frequency stability over the duration of the mission of $\delta f_0/f_0 < 2{\cdot}10^{-10}$ (f_0: nominal output frequency) within a 30-minute warm-up time. This could not be guaranteed with a state-of-the-art quartz oscillator.

Each USO consists of the physics package (rubidium resonance cell and lamp plus an SC-cut crystal) and six printed circuit boards integrated into an aluminum box (Faraday cage). The temperatures at three points in the physics package are monitored by analogue sensors. A lock indicator is provided to telemetry when the output is phase-locked to the Rb resonance frequency.

The mass of each unit is 1.9 kg, packed into a rectangular volume of approximately $17 \times 12 \times 12$ cm. The peak power consumption is less than 18.4 W during a warm-up time of $\sim$20 min, after which the power drops to a steady-state value $\sim$7.8 W (nominal values for the expected ambient temperature of 5 °C during Titan descent).

The actual drift stability determined during the DWE-USO qualification test program over an expanded range of temperatures ($-30° < T < 60°$) in vacuum (0.1 mbar) and ambient pressure was $\delta f_0/f_0 \leq 1.4 \cdot 10^{-9}$. This frequency stability exceeds the specified value, however, only for high temperatures ($T > 40°$), or when the USO needs more than the required 30 min to warm up ($T < -20°$). Under the expected environmental conditions at Titan, the error in the measurement of the line-of-sight velocity due to intrinsic oscillator instability should not exceed the originally specified goal of ± 6 cm s^{-1}. More detailed information about the mechanical, electrical and frequency characteristics of the DWE-USO are presented elsewhere (Bird *et al.*, 1997a,b).

5. Results of First In-flight Tests

The first in-flight checkout (F1) of the Huygens Probe payload occurred as planned on 23 October 1997, 8 days after the launch of the Cassini spacecraft. Only very minor problems were found in the quick-look data and a back-up checkout scheduled as contingency at launch +12 days was declared unnecessary.

An overview of the DWE data recorded during F1 is shown in Figure 7. The top two panels of Figure 7 show the recorded frequency f_R in the two redundant radio chains at the same scale, starting 40 min after the start of the checkout. The received signal level (AGC = automatic gain control) is shown for chains A and B in the bottom two panels. Both f_R and AGC are recorded at a sample time of 125 ms.

The initial 20 min are used for warming up the receivers and other Probe Support Equipment, including the DWE-RUSO. Measurements of frequency relevant to the nominal mission at Titan are possible only after an additional 20 min, which are allocated to the same warm-up process for the DWE-TUSO. This procedure is necessary only for the cruise checkouts. The nominal sequence of events during the actual mission at Titan are such that both DWE-USOs will be warmed up and stable at the moment the Huygens signal is acquired.

Whereas the TUSO/RUSO combination governs the recorded frequency in chain A, the standard oscillator frequency measurements in chain B are highly irregular.

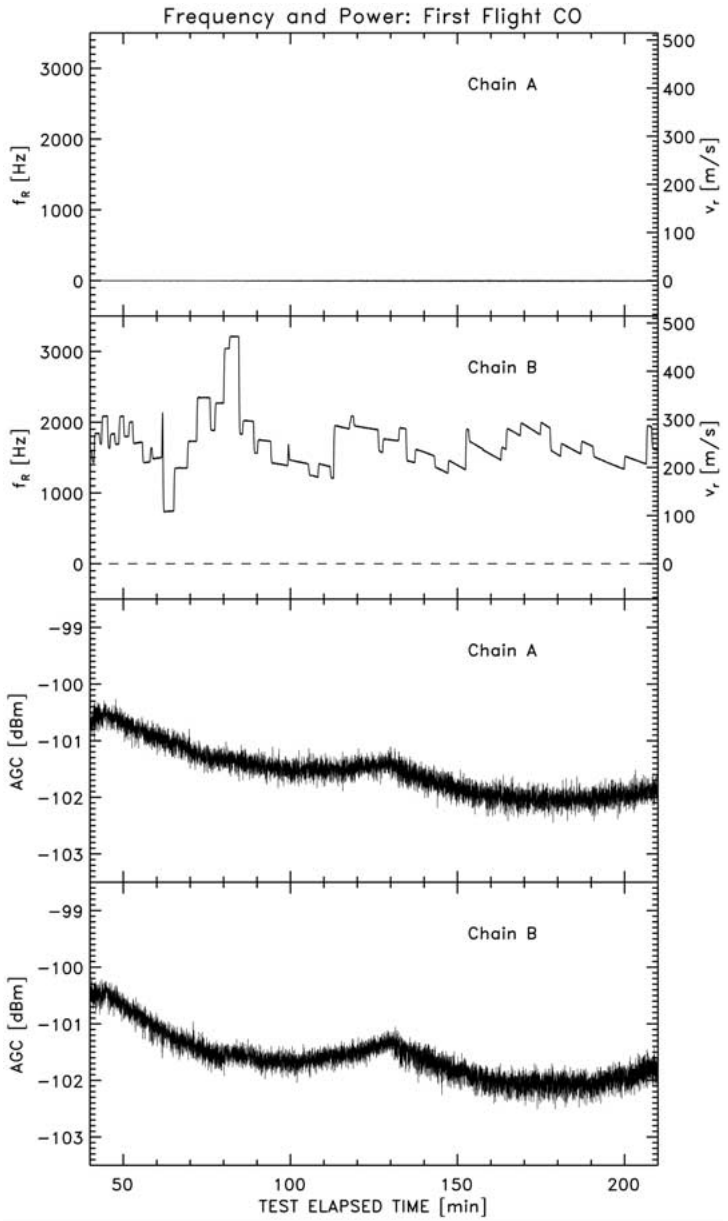

Figure 7. Huygens-DWE recorded frequency and signal level during the first in-flight checkout. Doppler data for radio chains A and B (upper 2 panels) are shown at the same scale (left ordinate: frequency in Hz; right ordinate: radial velocity in m s^{-1}). Chain A, driven by USOs, is frequency-stable. In contrast, chain B (no USOs) displays random oscillator drifts and discontinuities. The signal level (*AGC*) traces are virtually identical in the two chains (lower two panels). The first 40 min of the test (USO warm-up period) are not displayed.

The jumps in frequency, which arise from a thermal feedback loop driving a standard radio oscillator, are apparently random. Upon closer inspection of the intervals between jumps, it is found that the recorded frequency exhibits an unpredicable drift of instrumental origin. The frequency trace in chain A remains at its nominal value near 0 Hz during the entire checkout (Huygens is obviously not moving with respect to the receivers on the Orbiter). The large deviation from $f_R = 0$ in chain B is due to the imprecise output frequencies of the standard oscillators, which are constrained only to one part in 10^6. Unusual time profiles are seen in the signal level recordings (*AGC*), whereby both chains display the same irregular decrease by about 1 dB over the duration of the test. It was determined that this anomalous behavior, as subsequently verified by a special AGC-test after the first Venus flyby, was caused by solar radio noise entering the receivers through the sunward-pointed Cassini HGA. This interference essentially vanished after the Cassini spacecraft reached a solar distance of 2.7 AU, at which point the HGA was no longer needed as a sunshade and could be pointed at Earth for the remainder of the cruise phase.

It was determined rather late in the Probe pre-launch test program that a small, but annoying, spurious oscillation was present in the chain A frequency data. The amplitude of this oscillation was enhanced significantly after the Probe was mated to the Orbiter for launch configuration and was also seen to increase over the duration of the pre-launch checkout tests.

A high-resolution plot of the recorded frequency in radio chain A over a one-minute interval during F1, shown in the upper panel of Figure 8, reveals this spurious oscillation at a time when it had almost reached its maximum amplitude of 25 Hz peak-to-peak (p-p). The frequency of the spurious oscillation, as marked by the dominant peak in the power spectrum (Figure 8, second panel), is very constant at $f_s = 0.366$ Hz. This spectrum is the Fourier transform of the frequency time series in the test elapsed time interval from 50–200 min (Figure 7, upper panel). Harmonics of this frequency are also evident in the spectrum, albeit with considerably less power.

It was recognized soon after the discovery of the spurious oscillation that the unwanted modulation in the data could be eliminated by a Fourier filtering technique. The filtering procedure consists of re-assigning all spectral amplitudes above a given threshold to values at the noise level, selected randomly from the spectrum baseline. The third panel of Figure 8 shows such a 'filtered spectrum'. Although the two spectra look quite different, only 191 points of the original spectrum (from a total of 72 000) with amplitudes above the (arbitrary) cutoff at 10 Hz^2/Hz were reduced to noise levels by this process. The spectral power amplitudes at frequencies below 1 mHz, which are basically responsible for long-term drifting, were left unfiltered.

Finally, applying an inverse transform to the filtered spectrum, one obtains the filtered frequency trace in the time domain shown in the bottom panel of Figure 8. The spurious oscillation has virtually vanished. The filtered frequency measurements are centered at $\langle f_R \rangle \simeq -2.8$ Hz and the standard deviation is $\sigma_f \simeq 1.5$ Hz

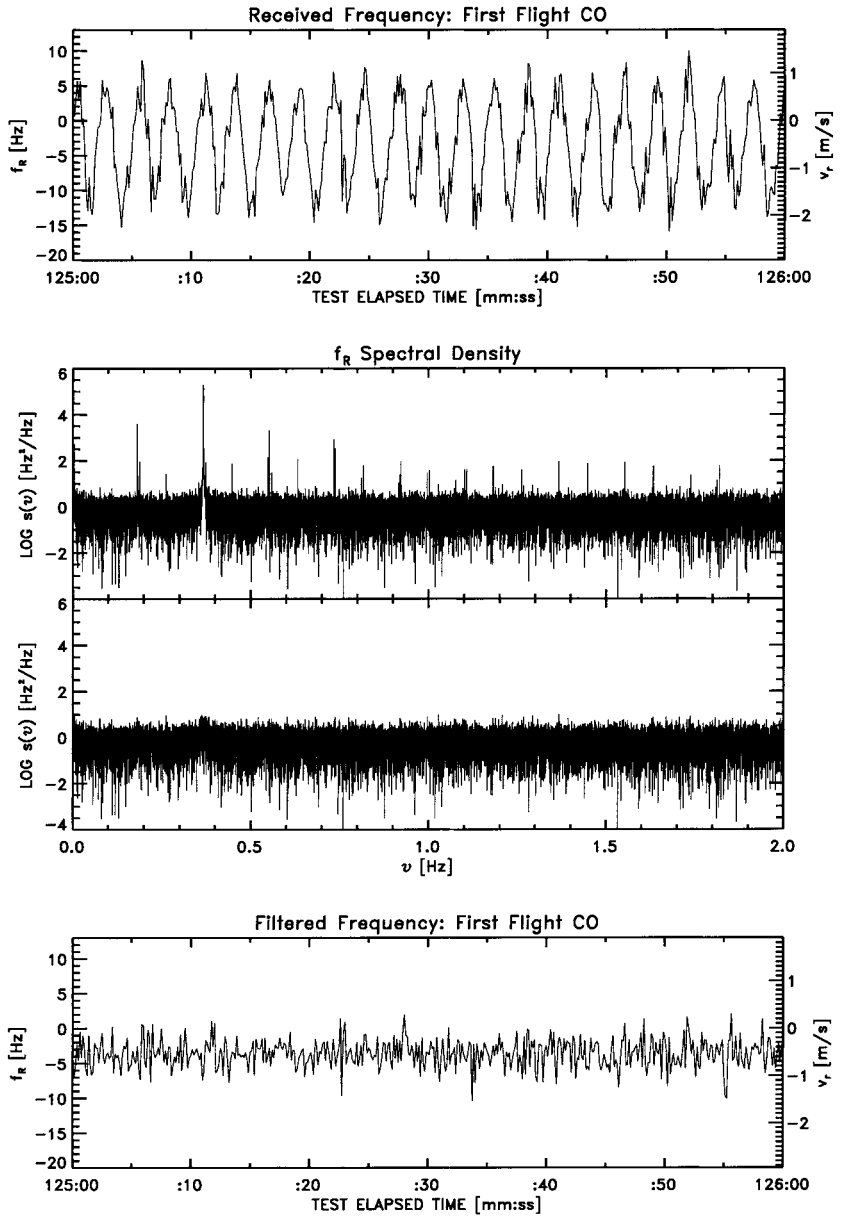

Figure 8. High-resolution frequency data from chain A during a one-minute interval beginning at 125 min. after start of test (upper panel). A power spectrum of the F1 frequency data from Figure 7 is shown in the second panel. The spurious oscillation, with amplitude ~20 Hz (p–p) and constant frequency $f_s = 0.366$ Hz, is evident in both data and spectrum. The spectral amplitudes of the original spectrum are reduced to the noise level at frequencies near f_s and its harmonics to produce a 'filtered spectrum' (third panel). The inverse transform of the filtered spectrum yields a frequency time series without the spurious oscillation (last panel).

for the data sampling rate rate of $f_d = 8$ Hz. The accuracy of the frequency measurement can be improved by increasing the integration time up to values near the natural time constant of the Probe system. This will be of the order of a few tens of seconds near the start of descent, decreasing to a few seconds just prior to impact (Bird *et al.*, 1997b). Assuming the data of Figure 8 are representative of the actual descent on Titan, we can expect to obtain a radial velocity measurement accuracy of the order of $\sigma_{\Delta V} \simeq \pm 6$ cm s^{-1} for a typical integration time of 2 s.

After considerable study, it has become known that the probable cause of the spurious oscillation is an internal USO signal used in a feedback loop to apply a small AC magnetic field to the rubidium cell. The oscillation frequency of this signal ($f_m = 135.63$ Hz) is derived from the 10 MHz USO output signal. When sampled by the receiver at the sampling rate f_d, an apparent spurious oscillation appears at the frequency $f_s = n \cdot f_d - f_m = 0.3663194$ Hz, where $n = 17$. Although the internal USO signal has the correct frequency to produce the spurious oscillation, it is still unclear why the amplitude grows from 8 to 25 Hz (p–p) over the duration of the checkout. Having monitored this disturbance for a total of 8 semiannual flight checkouts through September 2001, certain patterns in the amplitude of the spurious oscillation have emerged. Among these is a weak correlation between the received frequency offset and the oscillation amplitude that may be useful for final calibration of the DWE data from Titan. Still unknown, however, is the reason why the effect increased so dramatically when the Probe configuration was closed and then mated to the Orbiter for launch. Viewing the situation optimistically, this historical development implies that the oscillation amplitude may well be smaller after the Probe separates from the Orbiter and transmits remotely while descending through the atmosphere of Titan.

6. Probe Relay Test: Doppler Calibration

The DWE frequency measurement f_R used to determine the zonal winds on Titan is the difference between the Doppler shift of the received signal Δf and an offset frequency f_{off}. This offset frequency is comprised of an internal receiver reference frequency f_{ref} and the intrinsic offset frequencies of RUSO f_{off_R} and TUSO f_{off_T}, converted to S-band.

$$f_R = \Delta f - f_{off} \tag{9}$$

with

$$f_{off} = f_{ref} + f_{off\_R} - f_{off\_T} \tag{10}$$

In order to determine the absolute value of Δf, it is necessary to know the value of f_{off} to reasonably high precision. Atkinson (1990) demonstrated that it is possible, in principle, to conduct a Doppler wind measurement by tracking only the changes of f_R between successive samples, i.e. without knowledge of the absolute

value of the measured frequency. This approach, however, may not be feasible because of constraints on the geometry between Huygens and Cassini during the Titan descent.

According to the original mission plan, which was valid until July 2001, Cassini was to approach Titan at a velocity of -5.7 km s^{-1} during nearly the entire Huygens descent (negative velocity for decreasing distance). The carrier frequency measurement (DWE science data) would have consequently been blue-shifted by about 38.5 kHz with respect to the nominal 2040 MHz on chain A. Because this value is higher than the maximum trackable carrier frequency deviation in the receiver (± 30 kHz), the band pass can be tuned to either checkout mode ($f_{ref} = 0$ Hz) used for the regular in-flight checkouts or mission mode ($f_{ref} = 38.5$ kHz) for the mission.

This strategy was changed, however, after the above mentioned redesign of the Huygens mission with a high altitude Orbiter flyby. The new geometry greatly reduces the Cassini/Huygens range rate from the roughly constant -5.7 km s^{-1} to a nearly linear increase from -2.5 to $+1.6$ km s^{-1}. The resulting Doppler shift thus varies from about $+17$ to -11 kHz. Under this scenario the Huygens transmission from Titan would best be received in checkout mode. A switch to mission mode is undesired and, because of built-in precautions to default to mission mode if the signal is momentarily lost, must be inhibited by continually commanding the receiver to checkout mode.

The regular in-flight checkouts performed thus far ($f_{ref} = 0$ Hz) have revealed a nearly constant offset between TUSO and RUSO of $f_{off\_T} - f_{off\_R} \simeq -2.8$ Hz. It is unlikely that the RUSO and TUSO offsets would maintain their constant difference by drifting at exactly the same rate. A far more plausible conclusion is that both RUSO and TUSO output frequencies have not changed significantly since launch. On the other hand, it cannot be taken for granted that the value for the Doppler compensation in mission mode f_{ref} (never used in checkout mode) is set exactly to 38500.0 Hz.

An opportunity to calibrate the receiver frequency in mission mode and test the DWE instrumentation for the first time with a time-dependent Doppler shift occurred during the initial Probe Relay Test (PRT#1) conducted on 3/4 February 2000. The prime objective of PRT#1 was a flight calibration of the signal-to-noise measurement by the Automatic Gain Control (AGC), but the test also demonstrated that carrier lock on the dynamic signal could be maintained even for very low AGC levels and was declared a success from the DWE standpoint. Unfortunately, the test also demonstrated that the receivers were unable to demodulate the synthetic telemetry data. A more detailed analysis revealed a serious design flaw in the receiver that could only be circumvented with an extensive complete overhaul of the Huygens mission. A follow-up test (PRT#2) was performed aproximately one year later to better characterize the link performance as a function of the various signal parameters.

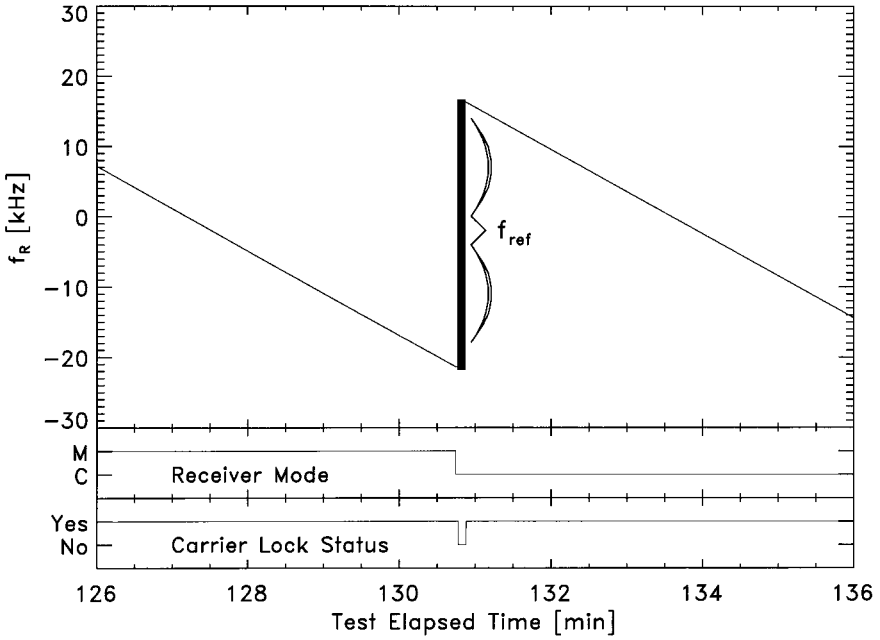

Figure 9. Upper panel: Measured frequency f_R during a 10 min interval about the switch from mission to checkout mode; Middle panel: Receiver Mode ('C' = checkout; 'M' = mission); Lower panel: Carrier Lock Status. The best fit value for $f_{ref} = 38\,504.2$ Hz was obtained from the vertical displacement of the two lines.

As illustrated in Figure 9, a direct measurement of f_{ref} could be obtained during the third Probe Relay Test (PRT#3) on 18 June 2001, scheduled primarily to verify the tracking capabilities of the carrier tracking loop.

Similar to the two previous PRTs, a simulated Huygens signal was uplinked to Cassini at various power levels from the Goldstone DSN station DSS 24. The Huygens Probe itself, including the TUSO, remained dormant. Correspondingly, the frequency offset for the PRT was $f_{off} = f_{ref} + f_{off\_R}$. The signal was received with the Cassini HGA and routed to the Huygens dedicated PSA.

The uplink frequencies were generated by a Hydrogen maser, the stability of which is superior to that of the DWE-USOs by about two orders of magnitude. For the tests on chain A with RUSO, the frequency was programmed to sweep over a range from $+78$ to -40 kHz around the nominal value of 2040 MHz. It was confirmed that the carrier loop bandwidth is ± 31 kHz. During these frequency sweeps, the band pass was switched instantaneously from mission to checkout mode.

The determination of f_{ref} was performed by comparing the frequency measurements before and after the mode switch (see lower panels of Figure 9). The switch itself led to a link interruption (Carrier Lock Status = 'no') of about 10 s. The frequencies measured before the switch were extrapolated using a linear regression

and the result compared with the post-switch frequency. The slopes of the pre- and post-switch Doppler traces (about 100 Hz s^{-1}) differed by less than 10^{-4}. A best fit was obtained for an internal reference frequency $f_{ref} = 38\,504.2$ Hz. The same procedure was applied to a second switch to checkout mode from the same test sequence. A mean value from these two measurements was $f_{ref} = 38\,504.1 \pm 0.2$ Hz. As mentioned earlier, the actual Huygens mission will now most probably be conducted with the receiver in checkout mode, rather than the Doppler-shifted mission mode. Nevertheless, the good agreement with the pre-launch calibration for f_{ref} and the excellent carrier lock performance during the series of PRTs do provide their small measure of encouragement for a successful DWE at Titan.

7. Conclusions

The Huygens Doppler Wind Experiment is designed to determine the direction and strength of Titan's zonal winds. The wind is measured over a height range from 0–160 km from its Doppler signature on the Probe's radio relay signal to the Cassini Orbiter. Similar Earth-based observations will be recorded in order to separate meridional from zonal drift motion. The necessary frequency stability of the Probe carrier signal and its measurement on the Orbiter is realized by using rubidium ultrastable oscillators. In spite of a slight imperfection due to a spurious oscillation of the frequency measurement, the DWE instrumentation is fully functional and capable of meeting the originally defined scientific goals. Final trajectory reconstruction and analysis of Probe dynamics will benefit from the DWE data, enhancing the overall scientific yield of the Huygens mission.

Acknowledgements

We thank R. Kohl and K.-P. Wagner (Astrium Telecommunications, Ottobrunn, Germany) for their continued efforts during the DWE-USO Program. This paper presents results of a research project partially funded by the Deutsches Zentrum für Luft- und Raumfahrt (DLR) under contract 50 OH 9803. Parts of the research described in this paper were carried out by the Jet Propulsion Laboratory, California Institute of Technology, under a contract with the National Aeronautics and Space Administration and by NASA's Goddard Institute for Space Studies.

References

Allison, M.: 1992, A preliminary assessment of the Titan planetary boundary layer. In: *Symposium on Titan* [ESA SP-338], pp. 113–118.

Allison, M., Del Genio, A. D. and Zhou, W.: 1994, Zero potential vorticity envelopes for the zonal-mean velocity of the Venus/Titan atmospheres, *J. Atmos. Sci.* **51**, 694–702.

Atkinson, D. H., Pollack, J. B. and Seiff, A.: 1990, Measurement of a zonal wind profile on Titan by Doppler tracking of the Cassini entry probe, *Radio Sci.* **25**, 865–882.

Atkinson, D. H., Ingersoll, A. P. and Seiff, A.: 1997, Deep winds on Jupiter as measured by the Galileo Probe, *Nature* **388**, 649–650.

Atkinson, D. H., Pollack, J. B. and Seiff, A.: 1996, Galileo Doppler measurements of the deep zonal winds at Jupiter, *Science* **272**, 842–843.

Atkinson, D. H., Pollack, J. B. and Seiff, A.: 1998, The Galileo Probe Doppler Wind Experiment: Measurement of the deep zonal winds on Jupiter, *J. Geophys. Res.* **103**, 22 911–22 928.

Bird, M. K.: 1997, Atmospheric attenuation of the Huygens S-Band radio signal during the Titan descent. In: *Huygens Science Payload and Mission* [ESA-SP 1177], pp. 321–335.

Bird, M. K., Allison, M., Atkinson, D. H., Asmar, S. W., Dutta-Roy, R., Edenhofer, P., Folkner, W. M., Heyl, M., Iess, L., Plettemeier, D., Preston, R. A., Tyler, G. L. and Wohlmuth, R.: 1997a, Rubidium ultra-stable oscillators at Titan: The Huygens Doppler Wind Experiment. In: *Scientific Applications of Clocks in Space* [JPL Publ. 97–15], L. Maleki (ed.), pp. 211–220.

Bird, M. K., Heyl, M., Allison, M., Asmar, S. W., Atkinson, D. H., Edenhofer, P., Plettemeier, D., Wohlmuth, R., Iess, L. and Tyler, G. L.: 1997b, The Huygens Doppler Wind Experiment. In: *Huygens Science Payload and Mission* [ESA-SP 1177], pp. 139–162.

Caldwell, J., Wu, N., Smith, P. H., Lorenz, R. D. and Lemmon, M. T.: 1996, Hubble Space Telescope imaging of Titan in 1995, *Bull. Amer. Astron. Soc.* **28**, 1132.

Combes, M., Vapillon, L., Gendren, E., Coustenis, A., Lai, O., Wittemberg, R. and Sirdey, R.: 1997, Spatially resolved images of Titan by means of adaptive optics, *Icarus* **129**, 482–497.

Coustenis, A.: 1990, Spatial variations of temperature and composition in Titan's atmosphere: Recent results, *Ann. Geophysicae* **8**, 645–652.

Coustenis, A. and Taylor, F.: 1999, *Titan: The Earth-like moon*, World Scientific Publ. Co., Singapore.

Del Genio, A. D., Zhou, W. and Eichler, T. P.: 1993, Equatorial superrotation in a slowly rotating GCM: Implications for Titan and Venus, *Icarus* **101**, 1–17.

Flasar, F. M.: 1998, The dynamic meteorology of Titan, *Planet. Space Sci.* **46**, 1125–1147.

Flasar, F. M., Allison, M. and Lunine, J. I.: 1997, Titan zonal wind model. In: *Huygens Science Payload and Mission* [ESA-SP 1177], pp. 287–298.

Flasar, F. M., Samuelson, R. E. and Conrath, B. J.: 1981, Titan's atmosphere: temperature and dynamics, *Nature* **292**, 693–698.

Folkner, W. M., Preston, R. A., Border, J. S., Navarro, J., Wilson, W. and Oestreich, M.: 1997, Earth-based radio tracking of the Galileo Probe for Jupiter wind estimation, *Science* **275**, 644–646.

Folkner, W. M., Woo, R. and Nandi, S.: 1998, Ammonia abundance in Jupiter's atmosphere derived from the attenuation of the Galileo Probe's radio signal, *J. Geophys. Res.* **103**, 22 847–22 855.

Fulchignoni, M. *et al.*: 1997, The Huygens Atmospheric Structure Instrument (HASI), In: *Huygens Science Payload and Mission* [ESA-SP 1177], pp. 163–176.

Griffith, C. A., Owen, T., Miller, G. A. and Geballe, T.: 1998, Transient clouds in Titan's lower atmosphere, *Nature* **395**, 575–578.

Griffith, C. A., Hall, J. L., and Geballe, T.: 2000, Detection of daily clouds on Titan, *Science* **290**, 509–513.

Hanel, R. *et al.*: 1981, Infrared observations of the Saturnian system from Voyager 1, *Science* **212**, 192–200.

Hinson, D. P. and Tyler, G. L.: 1983, Internal gravity waves in Titan's atmosphere observed by Voyager radio occultation, *Icarus* **54**, 337–352.

Hourdin, F., Talagrand, O., Sadourny, R., Courtin, R., Gautier, D. and McKay, C. P.: 1995, Numerical simulation of the general circulation of the atmosphere of Titan, *Icarus* **117**, 358–374.

Hubbard, W. B. *et al.*: 1993, The occultation of 28 Sgr by Titan, *Astron. Astrophys.* **269**, 541–563.

Hunten, D. M., Tomasko, M. G., Flasar, F. M., Samulson, R. E., Strobel, D. F. and Stevenson, D. J.: 1984, Titan, In: *Saturn*, T. Gehrels and M. S. Mathews (eds.), U. Arizona Press, Tucson, pp. 671–759.

Jaffe, L. D. and Herrell, L. M.: 1997, Cassini/Huygens scientific instruments, spacecraft, and mission, *J. Spacecraft Rockets* **34**, 509–521.

Kostiuk, T., Fast, K. E., Livengood, T. A., Hewagama, T., Goldstein, J. J., Espenak, F. and Buhl, D.: 2000, Direct measurement of winds on Titan, *Geophys. Res. Lett.*, **28**, 2361–2364.

Kunde, V. G. *et al.*: 2002, The Composite Infrared Spectrometer, *Space Sci. Rev.*, this issue.

Lebreton, J.-P. and Matson, D. L.: 1997, The Huygens Probe: science payload and mission overview. In: *Huygens Science Payload and Mission* [ESA-SP 1177], pp. 5–24.

Lebreton, J.-P. and Matson, D. L.: 2002, The Huygens Probe: Science, Payload and Mission. *Space Sci. Rev.*, **104**, 59–100.

Lindal, G. F., Wood, G. E., Holtz, H. B., Sweetnam, D. N., Eshleman, V. R. and Tyler, G. L.: 1983, The atmosphere of Titan: An analysis of the Voyager 1 radio occultation measurements, *Icarus* **53**, 348–363.

Lellouch, E., Coustenis, A., Gautier, D., Raulin, F., Dubouloz, N. and Frère, C.: 1989, Titan's atmosphere and hypothesized ocean: A reanalysis of the *Voyager 1* radio-occultation and IRIS 7.7-μm data, *Icarus* **79**, 328–349.

Lorenz, R. D., Smith, P. H. and Lemmon, M. T.: 1995, The search for clouds on Titan using HST imaging, *Bull. Amer. Astron. Soc.* **27**, 1107.

Lorenz, R. D., Lemmon, M. T. and Smith, P. H.: 1999, Evidence for clouds on Titan from HST WFPC-2, *Bull. Amer. Astron. Soc.* **31**, 1137.

Lunine, J. I., Flasar, F. M. and Allison, M.: 1991, Huygens Probe wind drift: science issues and recommendations, Internal Report to the Huygens Project.

Meier, R., Smith, B. A., Owen, T. C. and Terrile, R. J.: 2000, The surface of Titan from NICMOS observations with the Hubble Space Telescope, *Icarus* **145**, 462–473.

Pollack, J. B., Atkinson, D. H., Seiff, A. and Anderson, J. D.: 1992, Retrieval of a wind profile from the Galileo Probe telemetry signal, *Space Sci. Rev.* **60**, 143–178.

Seiff, A., Blanchard, R. C., Knight, T. C. D., Schubert, G., Kirk, D. B., Atkinson, D., Mihalov, J. D. and Young, R. E.: 1997, Wind speeds measured in the deep jovian atmosphere by the Galileo Probe accelerometers, *Nature* **388**, 650–652.

Smith, P. H., Lemmon, M. T., Lorenz, R. D., Sromovsky, L. R., Caldwell, J. J. and Allison, M. D.: 1996, Titan's surface, revealed by HST imaging, *Icarus* **119**, 336–349.

Sollazzo, C. *et al.*: 1997, Cassini/Huygens integrated data link report, *ESA-JPL-HUY-25999.*

Tokano, T., Neubauer, F. M., Laube, M. and McKay, C. P.: 1999, Seasonal variation of Titan's atmospheric structure simulated by a general circulation model, *Planet. Space Sci.* **47**, 493–520.

Tomasko, M. G. *et al.*: 1997, The Descent Imager/Spectral Radiometer (DISR) aboard Huygens, In: *Huygens Science Payload and Mission* [ESA-SP 1177], pp. 109–138.

Toon, O. B., McKay, C. P., Courtin, R. and Ackerman, T. P.: 1988, Methane rain on Titan, *Icarus* **75**, 255–284.

Tyler, G. L., Eshleman, V. R., Anderson, J. D., Levy, G. S., Lindal, G. F., Wood, G. E. and Croft T. A.: 1981, Radio science investigations of the Saturn system with Voyager 1: Preliminary results, *Science* **212**, 201–206.

Wenkert, D. D. and Garneau, G. W.: 1987, Does Titan's atmosphere have a 2-day rotation period?, *Bull. Amer. Astron. Soc.* **19**, 875.